Refereed Proceedings

The 13th International Conference on Fluidization - New Paradigm in Fluidization Engineering

Engineering Conferences International *Year* 2010

CFD SIMULATION OF A LIQUID-FLUIDIZED BED OF BINARY PARTICLES

Long Fan[*] John Grace[†]

Norman Epstein[‡]

[*]University of British Columbia

[†]University of British Columbia, Vancouver, Canada, jgrace@chbe.ubc.ca

[‡]University of British Columbia

CFD SIMULATION OF A LIQUID-FLUIDIZED BED OF BINARY PARTICLES

Long Fan, John R. Grace*, Norman Epstein
Department of Chemical & Biological Engineering, University of British Columbia,
2360 East Mall, Vancouver, Canada V6T1Z3

Abstract: The ability of computational fluid dynamics to predict the expansion and segregation of a binary solids mixture in a liquid-solid fluidized bed is investigated. Unsteady laminar flow is simulated by a modified two-dimensional Eulerian-Eulerian model in Fluent 6.3. The predictions are compared with experimental results for binary particles in the same narrow (1.00-1.18 mm) size range, but with different densities, 1600 and 1900 kg/m^3, fluidized by water (1). The voidages and heights of two layers which form, each dominated by one particle species, were found to be sensitive to small changes in particle properties (diameter, density, sphericity), as well as temperature (because of its effect on the water viscosity). As a result, agreement between simulations and experimental results depends on several incompletely characterized factors. Temperature via the water viscosity greatly influences heights and volume fractions of the two layers. Allowing for non-spherical particle shapes is also crucial in reconciling predictions and experimental data.

1. INTRODUCTION

Liquid-fluidized beds can classify binary particle systems when the two solid species differ in size, density and/or shape (2, 3). A number of empirical and semi-empirical models have been used to predict the behaviour of such systems, including predicting “inversion”, whereby one species reports to the bottom of the column at low superficial liquid velocities, but to the top at higher velocities. With the development of computer technology, computational fluid dynamics (CFD) simulation is becoming more and more useful. In fluidization, CFD has been applied predominantly to single particle species of uniform properties. However, its capability for binary particles in liquid-fluidized beds has received little attention (4-7).

* Corresponding author, Tel: +1-604-822-3121; fax: +1-604-822-6003. E-mail: jgrace@chbe.ubc.ca

In this paper, we investigate a liquid-solid system with binary particles. The operating conditions are chosen to match those in experiments by Galvin et al. (1), where liquid-solid fluidization was investigated in a Perspex tube of 50 mm diameter and 2000 mm height. Fluidizing water was supplied from a head tank to the base of the vessel via a uniformly porous distributor plate. Two species of particles, 0.139 kg of density 1600 kg/m^3 and 0.169 kg of density 1900 kg/m^3, were tested, both having the same 1.00-1.18 mm size range. The system was operated at superficial velocities of 0.031 to 0.058 m/s, in each case for 30 minutes to achieve dynamic equilibrium. The liquid was tap water at ambient conditions.

2. CFD MODEL

For our system, all particle Reynolds numbers, $\rho dU/\mu$, < 100. Turbulent model predictions for fluidized beds may be less consistent with experimental data than a laminar model unless an appropriate turbulence model with correct empirical constants and closures is chosen (8). Hence a laminar flow model was adopted. Each solid species was treated as a separate phase. To allow reasonable integration time, a two-dimensional, rectangular fluidized bed was modeled based on an unsteady state, Eulerian-Eulerian multiphase model with a time step of 0.001 s.

The unsteady-state, two-dimensional continuity and momentum equations for the liquid and the two solid phases are:

$$\frac{\partial}{\partial t}\left(\alpha_l \rho_l\right) + \nabla\left(\alpha_l \rho_l \vec{u_l}\right) = 0 \tag{1}$$

$$\frac{\partial}{\partial t}\left(\alpha_{s1} \rho_{s1}\right) + \nabla\left(\alpha_{s1} \rho_{s1} \overrightarrow{u_{s1}}\right) = 0 \tag{2}$$

$$\frac{\partial}{\partial t}\left(\alpha_{s2} \rho_{s2}\right) + \nabla\left(\alpha_{s2} \rho_{s2} \overrightarrow{u_{s2}}\right) = 0 \tag{3}$$

$$\frac{\partial}{\partial t}\left(\alpha_l \rho_l \vec{u_l}\right) + \nabla \cdot \left(\alpha_l \rho_l \vec{u_l}^2\right) = -\alpha_l \nabla p + \nabla \cdot \overline{\overline{\tau_l}} + \alpha_l \rho_l \vec{g} + K_{sl}\left(\overrightarrow{u_{s1}} - \vec{u_l}\right) + K_{sl}\left(\overrightarrow{u_{s2}} - \vec{u_l}\right) \tag{4}$$

$$\frac{\partial}{\partial t}\left(\alpha_{s1} \rho_{s1} \overrightarrow{u_{s1}}\right) + \nabla \cdot \left(\alpha_{s1} \rho_{s1} \overrightarrow{u_{s1}}^2\right) = -\alpha_{s1} \nabla p + \nabla p_{s1} + \nabla \cdot \overline{\overline{\tau_{s1}}} + \alpha_{s1} \rho_{s1} \vec{g} + K_{ls}\left(\vec{u_l} - \overrightarrow{u_{s1}}\right) + K_{ss}\left(\overrightarrow{u_{s2}} - \overrightarrow{u_{s1}}\right) \tag{5}$$

$$\frac{\partial}{\partial t}\left(\alpha_{s2} \rho_{s2} \overrightarrow{u_{s2}}\right) + \nabla \cdot \left(\alpha_{s2} \rho_{s2} \overrightarrow{u_{s2}}^2\right) = -\alpha_{s2} \nabla p + \nabla p_{s2} + \nabla \cdot \overline{\overline{\tau_{s2}}} + \alpha_{s2} \rho_{s2} \vec{g} + K_{ls}\left(\vec{u_l} - \overrightarrow{u_{s2}}\right) + K_{ss}\left(\overrightarrow{u_{s1}} - \overrightarrow{u_{s2}}\right) \tag{6}$$

where $$\overline{\overline{\tau}}_q = \alpha_q \mu_q \left(\nabla \cdot \vec{u}_q + \nabla \cdot \vec{u}_q^{\mathrm{T}} \right) + \alpha \left(\lambda_q - \frac{2}{3} \mu_q \right) \nabla \cdot \vec{u}_q \overline{\overline{I}} \quad (7)$$

These equations were solved by the FLUENT 6.3 CFD code based on the laminar flow option in double precision. Gambit (9) generated the grids. The kinetic theory of granular flow (10) was applied to both solid phases. The equation of Lun et al. (11) provided the granular bulk viscosity. The expression of Schaeffer (12) was used for friction viscosity, with an angle of internal friction of 30°. The restitution coefficient was 0.9 for all simulations.

The solids were initially treated as spherical particles, with the drag force between solid and liquid obtained from the equation of Gidaspow et al. (13). The solid-solid momentum exchange coefficient K_{ss} was calculated from the Syamlal-O'Brien symmetric model (14).

The sum of the volume fractions of the solid phases and liquid is unity, i.e.

$$\alpha_{s1} + \alpha_{s2} + \alpha_l = 1 \quad (8)$$

No-slip boundary conditions were imposed at all solid surfaces, but different boundary conditions had little influence on the simulations. Water was assumed to be introduced uniformly across the distributor as the entry boundary condition. The two solid phases were interspersed uniformly at time zero.

The size of the computational grid was fine enough to provide a grid-independent solution. The equations were discretized using the first-order upwind scheme and solved by the SIMPLE algorithm (15). The non-linearity in the phase momentum equations was dealt with by under-relaxation. When the residuals of all of the equations met the pre-established tolerance (10^{-3}), a converged solution was deemed to have been obtained.

3. CFD PREDICTIONS AND DISCUSSION

For simplicity, the expanded bed height was determined at the centre of the column. Simulated solid volume fractions were cross-sectional-averages after reaching steady state. The average diameter, 1.09 mm, was first assumed to apply to all particles, and the temperature (not reported by Galvin et al. (1)) was assumed to have been 20ºC. The simulation was first carried out for the smallest superficial velocity, 0.031 m/s, tested experimentally. In this case, the bed height achieved steady state after 150 s. The predicted solid volume fractions and experimental results, compared in Figure 1, are in reasonably good agreement.

Figure 2 shows that the simulated and experimental solid volume fractions for *U*=0.058 m/s led to significantly greater differences between the CFD predictions and experimental values. In particular, the experimental bed height was ~0.95 m, while the simulated one was only 0.6 m. To determine the cause of this large difference at the higher liquid velocity, we examined the influences of such particle properties as density, diameter and shape, as well as water temperature.

Since the particle diameter was in a range of 1.00-1.18 mm, we first explored the sensitivity to particle size by changing the diameter from 1.09 to 1.00 mm for both species, with the densities unchanged. While the predicted volume fractions of both types of particles were better than for a diameter of 1.09 mm, the improvement was too small to make a significant difference.

Reasoning that the particle densities may have been reported to only two significant figures*, the densities of the two species were next reduced from 1600 and 1900 kg/m^3 to 1550 and 1850 kg/m^3, respectively. The predicted volume fraction of lighter particles was again closer to the experimental predictions than for the original simulation, but, as for the previous case, the improvement was too small to make up for the discrepancy. Next we changed the density and diameter simultaneously to check their combined effect. The results (not shown here) indicated that the simulation of the lighter particles was improved, but there was no improvement for the heavier particles and too small an overall improvement.

Experiments (e.g. 17) have shown that deviation of a particle from a spherical shape causes more drag and therefore a decrease in terminal velocity. As a result, the expanded bed height for non-spherical particles is higher than for otherwise equivalent spherical particles. Many previous workers have correlated the drag coefficients of particles of non-spherical (including irregular) shapes. Here the sphericity was taken as 0.7 based on an estimate by Galvin (16). The drag coefficient equation of Haider and Levenspiel (18) was tried first, but gave unsatisfactory results. We next tried the relatively simple and accurate correlation of Tran-Cong et al. (18). This correlation requires the particle circularity (also referred to as surface sphericity), given by

$$c = \pi d_A / P_p \quad \text{where} \quad d_A = \sqrt{4A_p/\pi}\ , \quad d_n = \sqrt[3]{6V/\pi}\ ,$$

Since it was not reported by Galvin et al. (1), we used $d_A/d_n = 1.20$ and *c* = 0.7.

* We subsequently were told (16) that the densities were likely accurate to three significant digits.

Figure 3 compares the experimental data, as well as CFD predictions with the drag coefficient model of Gidaspow et al. (13) for spherical particles, with the predictions based on the drag correlation of Tran-Cong et al. (19) for non-spherical particles. Allowing for non-spherical particle shape clearly improved the simulation for this liquid-fluidization system, leading to an increase in predicted bed height of about 20%, with the volume fraction of lighter particles then in good agreement with experimental data. However, much more time (700 s) was required for the lighter particles to reach steady state. Moreover, allowance for non-spherical shape did not improve the volume fraction of heavier particles.

We next tested another approach to account for the non-spherical shapes where both species of particles were treated as oblate spheroids. Since the particle sizes were obtained by sieving, the 1.09 mm mid-size was taken as the diameter in the plane of symmetry, leading to a volume-equivalent diameter of 0.895 mm. The drag coefficient equation of Haider and Levenspiel (18) was then used. As shown in Figure 4, excellent agreement was obtained 500 s after initiating fluidization of a uniform mixture of the two species, with the excellent agreement applying not only to the lighter particles, but also to the heavier particles. We note, however, that the CFD model required a very long simulated time to approach steady state, with predictions corresponding to 1000 s less favorable than at 500 s.

Another possible cause of the difference between CFD predictions and the experimental results is the temperature, which significantly affects the viscosity of water. Escudié et al. (20) demonstrated that system temperature, often unreported, profoundly affects layer inversion predictions in liquid-fluidized beds of binary solids. Galvin et al. (1) did not report the experimental temperature in their paper. The above simulations all assumed a temperature of 20ºC, but Galvin (16) indicated that the temperature could have been as low as 13ºC. Figure 5 compares CFD predictions with experimental data for temperatures of 20, 13 and 4ºC. The predictions for 13ºC are better than for 20ºC. The results for 4ºC are in good agreement with the experiments, not only for the lighter particles, but also for the heavier ones. Clearly temperature exerts a significant influence on liquid-fluidized beds, and should always be controlled, measured and reported when publishing experimental results.

In addition to examining the sensitivity to particle properties (diameter, density, sphericity) and temperature, we also investigated the influence of turbulence. However, including turbulence in this system had little effect on the CFD predictions, too small to provide any significant improvement.

4. CONCLUSIONS

CFD predictions of longitudinal voidage profiles and bed expansion for water-fluidized beds of binary particles differing in density, but not diameter, showed varying agreement with experimental results. Predictions are strongly sensitive to temperature due to its influence on liquid viscosity, and to particle shape. Mean particle size and species density also influenced simulation results, though to too small a degree to explain the differences between the experimental and simulation results. It is important that those performing experiments on liquid-fluidized beds carefully measure and report particle shape and system temperature, so that accurate properties can be incorporated in predictive models.

ACKNOWLEDGEMENTS

Financial assistance from the Natural Sciences and Engineering Research Council of Canada (NSERC), the Canada Research Chairs program, and Syncrude Canada Limited are gratefully acknowledged.

NOTATION

A_p	projected area of particle, m^2	p	pressure, Pa
c	particle circularity, -	P_p	projected perimeter of particle, m
c_{fr}	coefficient of friction between two different solid phases, -	t	time, s
		T	assumed water temperature, ºC
d	particle diameter, m	U	superficial velocity, m/s
d_A	surface–equivalent-sphere diameter, m	V	particle volume, m^3
		α	volume fraction, -
d_n	volume-equivalent-sphere diameter or nominal diameter, m	λ	bulk viscosity, Pa·s
		μ	liquid viscosity, Pa·s
e	coefficient of restitution for particle-particle collisions, -	ρ	density, kg/m^3
		τ	shear stress, Pa
g	acceleration of gravity, m/s^2	*Subscripts*	
$g_{0,ss}$	radial distribution function between particles, -	l	liquid phase
		q	either liquid or solid phase
I	stress tensor, -	s	solid phase
K	interphase exchange coefficient, -		

REFERENCES

(1) Galvin, K.P., Swann, R., and Ramirez, W.F. (2006). “Segregation and dispersion

of a binary system of particles in a fluidized bed." *AIChE J*. 52, 3401-3410.
(2) Epstein, N. (2005). "Teetering." *Powder Tech*. 151, 2-14.
(3) Escudié, R., Epstein, N., Grace, J.R., and Bi, H.T. (2006). "Effect of particle shape on liquid-fluidized beds of binary (and ternary) solids mixtures: segregation vs. mixing." *Chem. Eng. Sci*. 61. 1528-1539.
(4) Syamlal, M., and O'Brien, T.J. (1988). "Simulation of granular layer inversion in liquid fluidized beds." *Int. J. Multiphase Flow*. 14(4), 473-481.
(5) Howley, M.A., and Glasser, B.J. (2002). "Hydrodynamics of a uniform liquid-fluidized bed containing a binary mixture of particles." *Chem. Eng. Sci*. 57, 4209-4226.
(6) Reddy, R.K., and Joshi, J.B. (2009). "CFD modeling of solid-liquid fluidized beds of mono and binary particle mixtures." *Chem. Eng. Sci*. 64, 3641-3658.
(7) Malone, K.F., Xu. B.H., Fairweather, M. 2007. Numerical investigation of the layer-inversion phenomenon in binary solid liquid fluidized beds. in Fluidization 12, ed. X. Bi, F. Berruti and T. Pugsley, 2007, Harrison, Canada. 297-304.
(8) Cornelissen, J.T., Taghipour, F., Escudié, R., Ellis, N., and Grace, J.R. (2007). "CFD modelling of a liquid-solid fluidized bed." *Chem. Eng. Sci*. 62, 6334-6348.
(9) FLUENT Inc., (2003). *FLUENT 6.1 User's guide*. FLUENT Inc., Lebanon, NH.
(10) Gidaspow, D. (1994). *Multiphase Flow and Fluidization*. Academic Press, London.
(11) Lun, C.K.K., Savage, S.B., Jeffrey, D.J., and Chepurniy, N. (1984). "Kinetic theories for granular flow: inelastic particle in Couette flow and slightly inelastic particles in a general flow field." *J. Fluid Mech*. 140, 223-256.
(12) Schaeffer, D.G. (1987). "Instability in the evolution equations describing incompressible granular flow." *J. Differential Equations*. 66, 19-50.
(13) Gidaspow, D., Bezburuah, R., and Ding, J. (1992). "Hydrodynamics of circulating fluidized beds, kinetic theory approach." *Fluidization VII*, ed. Potter, O.E., Nicklin, D.J. Engineering Foundation, New York, 75-82.
(14) Syamlal, M. (1987). *The particle-particle drag term in a multiparticle model of fluidization*, DOE/MC/21353-2373, DE87 006500.
(15) Patankar, S.V. (1980). *Numerical Heat Transfer and Fluid Flow*. New York, McGraw Hill.
(16) Galvin, K.P. (2009). University of Newcastle, Australia, *Personal communication*.
(17) Pettyjohn, E.S., and Christiansen, E.R. (1948). "Effect of particle shape on free-settling rates of isometric particles." *Chem. Eng. Prog*. 44, 157-172.
(18) Haider, A., and Levenspiel, O. (1989). "Drag coefficient and terminal velocity of spherical and non-spherical particles." *Powder Tech*. 58, 63-70.
(19) Tran-Cong, S., Gay, M., and Michaelides, E. (2004). "Drag coefficients of irregularly shaped particles." *Powder Tech*. 139, 21-32.
(20) Escudié, R., Epstein, N., Grace, J.R., and Bi, H.T. (2006). "Layer inversion phenomenon in binary-solid liquid-fluidized beds" *Chem. Eng. Sci*. 61, 6667-6690.

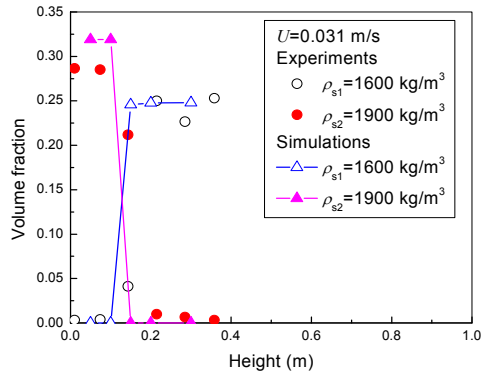

Figure 1. Comparison of predicted and experimental volume fractions for *U*=0.031 m/s. Temperature is assumed to be 20ºC.

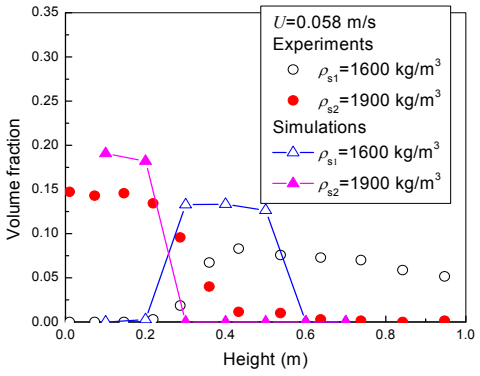

Figure 2. Comparison of predicted and experimental volume fractions for *U*=0.058 m/s, Temperature is assumed to be 20ºC.

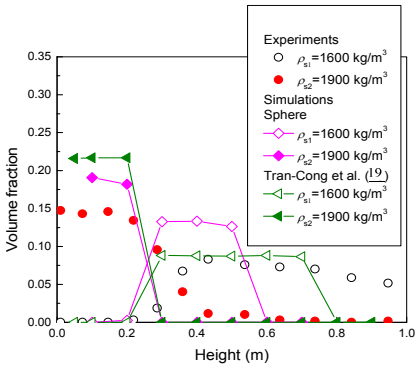

Figure 3. Comparison of simulated volume fractions from Tran-Cong. (19) drag model for sphericity=0.7, drag coefficient for spheres, with corresponding experimental data; *T*=20ºC.

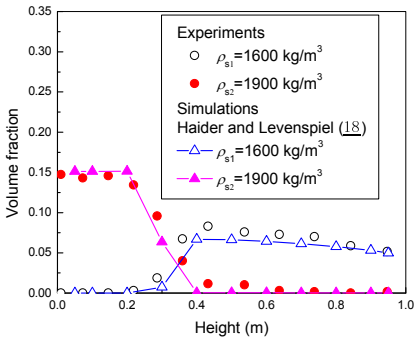

Figure 4. Comparison of experimental data for oblate spheroids of sphericity 0.7 (1) with CFD simulations 500 s after start-up as a uniform mixture using Haider and Levenspiel drag model (18). *T*=20ºC.

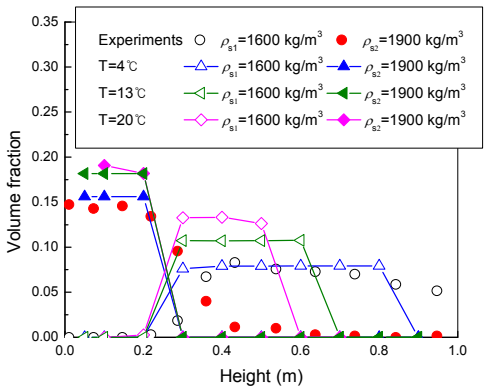

Figure 5. Influence of temperature on volume fractions of both particle species.

KEYWORDS

particle properties, CFD, binary particles, liquid-solid fluidization